

# BREAKDOWN CHARACTERIZATION IN 805 MHz PILLBOX-LIKE CAVITY IN STRONG MAGNETIC FIELDS\*

A. Kochemirovskiy, University of Chicago, IL, 60637, USA

D. Bowring, K. Yonehara, A. Moretti, D. Peterson, Fermilab, Batavia, IL, 60510, USA

G. Kazakevich, G. Flanagan, Muons, Inc. Batavia, IL, 60510, USA

M. Chung, UNIST, Ulsan 689-798, Korea

Y. Torun, B. Freemire, P. Hanlet, IIT, Chicago, IL, 60616, USA

## Abstract

RF Breakdown in strong magnetic fields has a negative impact on a cavity performance. The MuCool Test Area at Fermilab has unique capabilities that allow us to study the effects of static magnetic field on RF cavity operation. We have tested an 805 MHz pillbox-like cavity in external magnetic fields up to 5 T. Results confirm our basic model of breakdown in strong magnetic fields. We have measured maximum achievable surface gradient dependence on external static magnetic field. Damage inspection of cavity walls revealed a unique observed breakdown pattern. We present the analysis of breakdown damage distribution and propose the hypothesis to explain certain features of this distribution.

## INTRODUCTION

Muon ionization cooling channel designs require RF cavities to be operated in strong magnetic fields up to several Tesla [1, 2]. RF cavity performance is limited by breakdown: current discharge across a cavity accompanied by an abrupt drop in stored energy, light and x-ray emission, and a transient increase in vacuum pressure. It has been previously experimentally demonstrated that in strong magnetic fields the breakdown rate increases [3].

A model has been proposed which explains the effects of strong magnetic fields on breakdown-related cavity damage [4]. In the presence of a strong, solenoidal magnetic field, field-emitted electrons are focused into "beamlets" with current densities of  $10^3 - 10^5 \text{ A/m}^2$  at impact site. Space charge effects prevent further increase in beamlet current density above 0.5 T. These beamlets persist over multiple RF cycles and, through their impact on cavity surfaces, cause pulsed heating, cyclic material fatigue, and eventual breakdown. This type of damage may lead to increased breakdown probability. Materials with higher radiation length might be less prone to cyclic fatigue under such circumstances.

### Cavity Design and Instrumentation

The cavity used in this study was designed to operate wither under vacuum or filled with high-pressure gas, in order to study the role of gas pressure in the suppression of breakdown [5]. Due to this flexibility, the cavity was described as "a cavity for all seasons". The walls of so-called All Seasons Cavity (ASC) are fastened with bolts

and aluminum seals, allowing for relatively easy assembly and disassembly. The experimental goals of ASC program included determination of maximum achievable gradient for external magnetic fields between zero and five Tesla for cavity pressures between  $10^{-8}$  Torr and 100 atmospheres, optimization conditioning scheme for stable cavity performance at high gradients, assessment of different cavity wall materials such as copper, aluminum, beryllium [6, 7]. This paper presents results from vacuum operation of the ASC.

Figure 1 shows the cross section of the cavity with simulated electrical field distribution. The cavity was designed with two thick copper plated ( $25 \mu\text{m}$ ) detachable end plates. Flat thin Al gaskets were used to make RF and vacuum seal. Coaxial capacitive coupling was used for power transmission into the cavity. The list of RF properties of ASC is presented in Table 1.

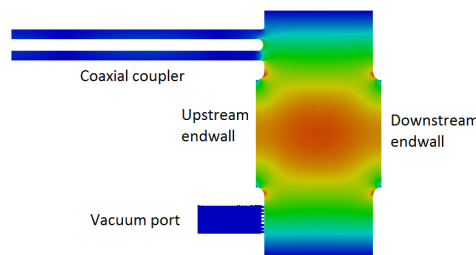


Figure 1: Cross section of ASC with electric fieldmap simulated in Omega3p.

Table 1: RF Properties of the Cavity

Parameter	Value
Frequency	810.4 MHz
$Q_0, Q_L$	28000, 15500
Coupling constant, $\beta$	0.8
Gap length	14.5 cm
Base vacuum pressure	$3 \times 10^{-8}$ Torr
Pulse length	30 $\mu\text{s}$
Stored energy at 20 MV/m	5 Joules
Rep rate	1Hz

### Instrumentation and Data Acquisition

Fermilab's MuCool Test Area (MTA) is a unique facility, built specifically to test RF cavities' performance in strong magnetic fields [8]. ASC cavity instrumentation included

\* Work supported in part by DOE STTR grant DE-FG02-08ER86352 and by Fermilab Research Alliance, LLC under Contract No. DE-AC02-07CH11359

the following items: LecroyWR625Zi oscilloscope with 0.1 ns sampling rate recorded electric pickup signal, reflected RF power from two directional couplers, NaI crystal radiation detector. Tektronix TDS5104 oscilloscope with 0.8 ns sampling rate was used to record forward and reflected RF power values. The value of external magnetic field was measured through the solenoid current. Figure 2 shows example of 2 waveform captures on the Lecroy scope of normal and breakdown event.

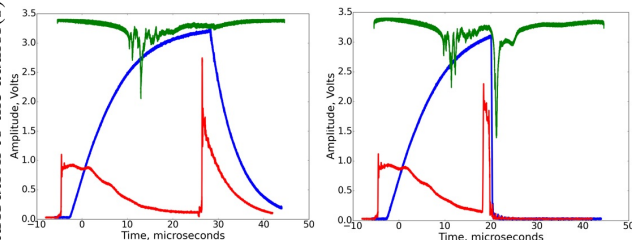


Figure 2: Envelope of pickup signal (blue), NaI radiation detector (green), reflected power (red) for normal event (left) and breakdown event (right). The peak-to-peak calibration constant for electric pickup signal is 7.44 MV/m per 1V.

## RF MEASUREMENTS

Initial evaluations of ionization cooling channel efficiencies give the maximum allowable spark rate as one spark in  $10^5$  RF pulses. In this paper, the “maximum achievable gradient” is the gradient at which the spark rate is below  $10^{-5} \pm 30\%$ . Table 2 presents the maximum achievable gradient for a given applied magnetic field. To measure the peak surface electric field, coaxial pickup signal was used and calibrated using Comsol fieldmap simulation package. The gradient vs.  $B$  behavior described in Table 2 is consistent with the predictions in [1]: the peak surface electric field above  $B \approx 0.25$  is approximately 20% lower than that at  $B = 0$  T, and this peak surface electric field is roughly constant for  $B \geq 0.25$  T.

Table 2: Maximum Achieved Peak Surface Gradients in External Static Solenoidal Magnetic Field

Magnetic field, T	Peak Surface Gradient, MV/m
0.00	$25.0 \pm 1.2$
0.25	$20.5 \pm 1.0$
0.50	$20.5 \pm 1.0$
1.00	$20.5 \pm 1.0$
3.00	$20.0 \pm 1.0$
4.00	$20.5 \pm 1.0$
5.00	$21.0 \pm 1.1$

## Damage Inspection

A clean room-compatible portable inspection system was used to characterize breakdown damage on cavity surfaces. It consists of a flatbed scanner with  $10^5$  pixels per  $\text{mm}^2$  and a

digital VHX-100K microscope with 3D imaging capabilities. After its final high-power run in February of 2014, the cavity was disassembled and inspected using this system. The damage was accumulated during runs with magnetic fields and surface gradients mentioned in Table 2. Data from this inspection system is presented in the next section.

The ASC’s RF surface is copper-plated stainless steel. This surface preparation differs from that of other cavities tested in the MTA, whose surfaces were machined, bulk copper. The difference in surface preparation may explain why the ASC’s performance - when compared with the performance of other cavities tested in the MTA - is more consistent with our model of RF breakdown in strong magnetic fields. The modular cavity walls are chemically polished and prepared using best practices from SRF, and so should be the clearest demonstration of the effects of surface preparation on RF breakdown rates.

## CHARACTERIZATION OF BREAKDOWN DAMAGE

Approximately 200 breakdown damage sites were observed on each flat cavity wall. Digital micrographs of typical breakdown damage sites are shown in Fig. 3. The volume of melted copper in Fig. 3 is estimated to be  $0.1 \text{ mm}^3$ . The energy required to melt this much copper is 0.8 J, the stored energy of the cavity at 20 MV/m is 5 J.

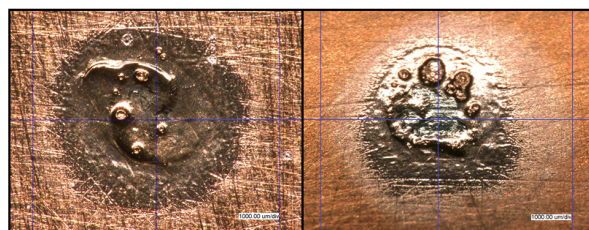


Figure 3: Microscopic images of typical breakdown pits. Diameter of each pit is around 1mm.

The cavity walls were scanned at  $10^5$  pixels per  $\text{mm}^2$ . A computer vision algorithm was used to identify breakdown sites in these scanned images. The coordinates of each identified breakdown site are plotted in Fig. 4.

There appears to be a one-to-one correspondence between damage on the upstream and downstream cavity walls. Figure 5 shows an example of matching pattern of four pits on opposing endwalls. This suggests that in the All-Seasons Cavity, breakdown sparks cause damage on the upstream and downstream cavity walls simultaneously.

Certain dominant pit orientations in XY plane were measured. Figure 6 shows the histogram of pit pairs orientations in plane perpendicular to cavity axis. The distribution appears to be bimodal, with two peaks located at 60 and 150 degrees. The average pit offset (the distance between two pits within a pair) was measured to be  $3.5 \pm 0.5$  mm.

We propose a hypothesis to explain the origin of preferable orientations of pit pairs. Dark current electrons emitted

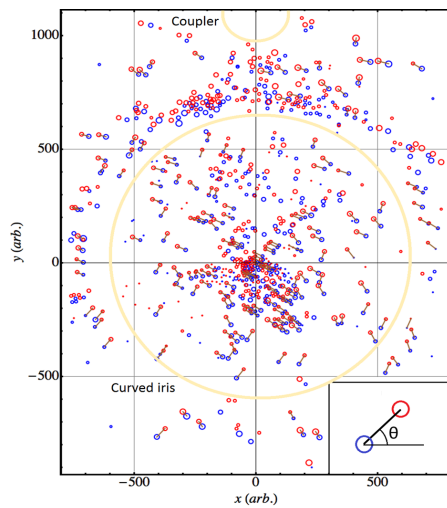


Figure 4: Distribution of breakdown pits on two opposing endplates. Red pits correspond to upstream endplate, blue - to downstream one. Corresponding pairs are connected with lines.

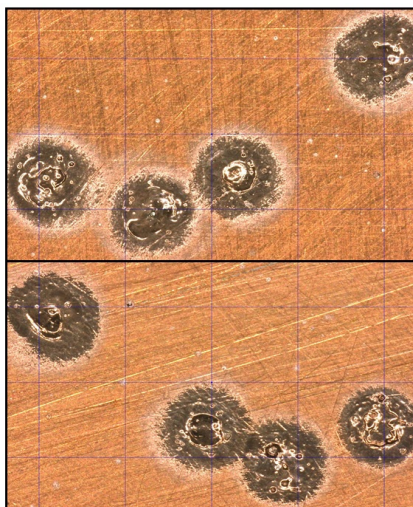


Figure 5: Corresponding damage pattern of four breakdown pits on opposing upstream (top) and downstream (bottom) endwalls. The diameter of each pit is around 1mm.

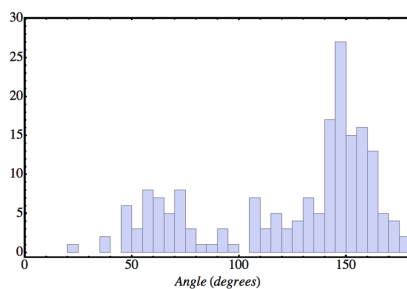


Figure 6: Histogram of pit orientation angles.

from cavity walls tend to follow magnetic field lines. According to our model of breakdown, focused beamlets of electrons create surface conditions for arc formation. Our assumption is that in strong magnetic fields arc trajectories follow trajectories of dark current beamlets. Binomial distribution of pit orientation, therefore, could arise from cavity runs under different external magnetic fields.

## CONCLUSION

We measured maximum achievable gradients for the set of external magnetic field values. Results are consistent with our expectations based on model mentioned in introduction. We established one-to-one correspondence between breakdown damage pits on opposing endwalls, obtained during runs with external magnetic field present. Our hypothesis indicates that magnetic field, focusing the dark current electrons, might be responsible for binomial pit orientation pattern. To prove our hypothesis, more systematic study is needed. Ideally, we would prefer to be able to disassemble the cavity and inspect breakdown damage after each run with certain conditions. These issues are addressed by an ongoing experimental program in the MTA [9].

## ACKNOWLEDGEMENT

This research used resources of the National Energy Research Scientific Computing Center, which is supported by the Office of Science of the U.S. Department of Energy under Contract No. DE-AC02-05CH11231. We would like to thank Lixin Ge for her assistance with Track3p code suite and Rol Johnson for his support.

## REFERENCES

- [1] R. Palmer et al., "Muon Collider Design", AIP Conf. Proc. 441 (1998) 183.
- [2] A. Blondel et al., "MICE, The International Muon Ionization Cooling Experiment", TUPFI046, IPAC'13.
- [3] A. Moretti et al., "Effects of high solenoidal magnetic fields on rf accelerating cavities", Phys.Rev. ST Accel.Beams 10 (2005) 072001.
- [4] D. Stratakis et al., "Effects of external magnetic fields on the operation of high-gradient accelerating structures", Nucl. Inst. Meth. A 620 (2010), 147-154.
- [5] B. Freemire et al., "High Powered Beam Test of a Dielectric Loaded High Pressure Gas Filled RF Cavity", IPAC'15, 2860 - WEPTY049.
- [6] G. Kazakevich et al., "Multi-purpose 805 MHz Pillbox RF Cavity for Muon Acceleration Studies", PAC'11, TUP092.
- [7] G. Kazakevich et al., "Conditioning and Future Plans for a Multi-purpose 805 MHz Pillbox Cavity for Muon Acceleration", IPAC'12, THPPC032.
- [8] Y. Torun, "MuCool Test Area Update", IPAC'15, 3767 - WEPTY053.
- [9] D. Bowring et al., "RF Breakdown of 805 MHz Cavities in Strong Magnetic Fields", IPAC'15, 3218 - MOAD2.